35th Annual International Conference of the IEEE EMBS
Osaka, Japan, 3 - 7 July, 2013

# Classification of Stand-to-Sit and Sit-to-Stand Movement from Low Frequency EEG with Locality Preserving Dimensionality Reduction

Thomas C. Bulea, *Member, IEEE,* Saurabh Prasad, *Member, IEEE,* Atilla Kilicarslan, and Jose L. Contreras-Vidal, *Senior Member, IEEE*

*Abstract*— **Recent studies have demonstrated decoding of lower extremity limb kinematics from noninvasive electroencephalography (EEG), showing feasibility for development of an EEG-based brain-machine interface (BMI) to restore mobility following paralysis. Here, we present a new technique that preserves the statistical richness of EEG data to classify movement state from time-embedded low frequency EEG signals. We tested this new classifier, using cross-validation procedures, during sit-to-stand and stand-to-sit activity in 10 subjects and found decoding accuracy of greater than 95% on average. These results suggest that this classification technique could be used in a BMI system that, when combined with a robotic exoskeleton, can restore functional movement to individuals with paralysis.**

## I. Introduction

Electroencephalography (EEG) is a method for imaging brain activity by measuring the electrical activity of pyramidal neurons in the superficial layers of the brain from electrodes placed on the scalp. While EEG recordings possess high temporal resolution, the potentials are a linear combination of many current sources, resulting in poor spatial resolution (volume conduction). Yet, the noninvasive nature of scalp EEG makes it an attractive candidate for use in brain-machine interfaces (BMIs). BMIs have been the subject of intensifying research over the past decade [1-3] and have been deployed in a wide range of applications, including control of computer cursors, powered wheelchairs, and assistive robots. BMIs are incorporated into rehabilitation therapy to either train the central nervous system to produce more normal activity, or to control a device that assists movement thereby producing sensory input that induces plasticity to restore motor control [2]. Finally, BMIs can be used to control prosthetic limbs or powered exoskeletons to restore functional mobility to amputees or individuals with paralysis.

The key component of a BMI for restoration of movement is the algorithm that translates brain signals into useful commands. One approach is to infer limb movement from the recorded neural signals. Many techniques have been investigated for this decoding task [4] including the Weiner filter, Kalman Filter, unscented Kalman filter, particle filter, artificial neural networks, and finite state approaches. A majority of these studies have applied these techniques to decoding motion of the upper extremity, such as reaching and grasping, from invasive neural recording such as electrocorticographic (ECoG) or local field potentials [5-7], while some studies demonstrate the feasibility of utilizing noninvasive EEG for these purposes in humans [8,9]. Extension of noninvasive neural decoding to the lower extremity offers great potential to BMIs for rehabilitation, since recovery of independent mobility after paralysis can greatly improve quality of life. Recent work has demonstrated the ability to decode lower extremity limb motion from scalp EEG [10,11]. While such decoding is useful for rehabilitation and motor recovery, individuals with paralysis or amputations could benefit from methods that classify the desired action in a more discrete fashion. For example, a BMI for controlling a robotic exoskeleton that restores walking mobility need not decode the exact desired trajectory of the limb; instead, the BMI must only decode the intent of the user (e.g., stand, walk, turn, stop, etc.). Once intent is established, internal controls of the exoskeleton can execute the desired movement.

Here we present a new strategy for EEG classification to infer user action from brain activity during sit-to-stand and stand-to-sit tasks. We employ a locality preserving dimensionality reduction technique coupled with a statistical classifier to determine the current state of the user from offline analysis of scalp EEG recordings.

## II. Methods

### A. Classifier Algorithm

A Gaussian mixture model (GMM) seeks to represent arbitrary statistical distributions in the feature space via a summation of multiple Gaussian distributions, termed components or modes. The shape of the resulting probability density function depends on the number of mixture components ($K$), and the mixing weight, mean, and covariance matrix of each component. The determination of $K$ is critical to successful implementation of GMMs for classification. The Bayes information criterion (BIC) has been reported as an effective metric for determining $K$ [12]. Once the value of $K$ has been determined, the other parameters of the GMM can be estimated by the expectation-maximization algorithm [13].

One drawback for use of GMMs is the size of the parameter space that must be learned, which can be calculated as $K*(1 + d*(d - 1)/2) + K*d$, where $d$ is the

This work was supported by the National Institute of Neurological Disorders and Stroke (NINDS) grant # R01NS075889-01.

T.C. Bulea is with the Functional and Applied Biomechanics Section at the National Institutes of Health, Bethesda, MD 20892 and the University of Houston, Houston, TX 77204. (email: thomas.bulea@nih.gov).

S. Prasad, A. Kilicarslan, and J.L. Contreras-Vidal are with the University of Houston, Houston, TX 77204 (e-mail: sprasad2@uh.edu, akilica2@uh.edu, jlcontreras-vidal@uh.edu ).

dimensionality of the data to be fit. It is common to include 10 lags of past EEG data in the feature matrix for neural decoding [10,11]. To fit a GMM with $K = 10$ components to a feature matrix constructed from 32 channels of EEG requires learning a parameter space of dimension $6.2 \times 10^5$, a task which is often impractical given the limited time and training data available from EEG studies. Many techniques for dimensionality reduction have been evaluated in BMI, with the most popular being genetic algorithm (GA), principal component analysis (PCA) and linear discriminant analysis (LDA) [4]. These methods have shown promising results, however these data reduction techniques have some limitations. In the case of PCA and LDA, the underlying assumption is that class-conditional data are Gaussian. Yet, scalp recorded EEG data represent a mixture of millions of neural inputs. Thus, it is likely that EEG data recorded for the purpose of determining user intent (e.g. sit or stand) will be contaminated by other neural activity. Therefore, we hypothesize that the statistical distribution of a given class will be multimodal, and thus, classifiers such as GMMs are well suited to classify user intent from EEG data. Evidence from prior studies indicates that utilization of a locality preserving dimensionality reduction, such as local Fisher's discriminant analysis (LFDA), improves performance of GMMs compared to traditional data reduction techniques [12]. LFDA combines LDA with a linear manifold learning technique to obtain between-class separation in the reduced dimension projection space while preserving the within class structure found in the original space. LFDA seeks to find a projection that preserves local neighborhood information, thereby ensuring that the underlying structure of the data distribution is preserved in a lower dimensional subspace. This is accomplished by deploying local between-class and within-class scatter matrices which are scaled by the distance between a given data point and its $k_{nn}$-nearest neighbor (the value of $k_{nn}$ must be optimized for a given data set). These local scatter matrices are used to define Fisher's ratio. The transformation matrix $T_{lfda}$, which projects the original data set into the reduced dimensional space, is then found by maximizing a modified form of Fishers ratio as in [12].

### *B. Experimental Setup and Data Collection*

Ten healthy adults (6 male, 4 female) with no history of neurological disease participated in the study after giving informed consent. This study protocol was approved by the Institutional Review Board at the University of Houston. Participants were asked to complete sit-to-stand and stand-to-sit tasks as follows. Participants were asked to stand quietly in an upright posture for 15 seconds. Next, an audio cue (beep) was given at which point the participant transitioned from the standing to a seated posture. The seated posture was held for a period ranging from 3-10 seconds, after which a second audio cue was given to initiate the transition from sit-to-stand. The standing posture was held for 3-10 second interval, at which point the process was repeated until 20 transitions (10 of each) were completed.

Time-locked kinematic, electromyography (EMG), and EEG data were collected simultaneously using a previously developed data collection system [14]. Inertial sensing units (APDM, Inc., Portland, OR) containing triaxial magnetometers, accelerometers, and gyroscopes sampled at 128 Hz were mounted bilaterally on the foot, shank, and thigh, and on the lower back, sternum, and head. Surface EMG (Biometrics, Ltd, Ladysmith, VA) was recorded at 1000 Hz bilaterally from the tibialis anterior, gastrocnemius, biceps femoris, and vastus lateralis. Whole scalp, active electrode, 64-channel EEG (Brain Products, GmbH, Morrisville, NC) were collected at 1000 Hz and labeled by the 10-20 international system.

### *C. Signal Preprocessing*

All data analysis, classifier optimization and evaluation were performed off-line using custom software in Matlab (Mathworks, Natick, MA). Peripheral EEG channels susceptible to eye blinks and facial/cranial muscle activity were removed for offline analysis (all channels labeled Fp, AF, FT, T, TP, O, and P7-8, PO7-10). Time traces of the remaining channels were visually inspected to assure no irregularities were present. EEG signals were decimated to 100 Hz and then band pass filtered with a zero phase, 3rd order Butterworth filter from 0.1-2 Hz. The EEG data were then standardized by channel by subtracting the mean and dividing by the standard deviation. Finally, a time-embedded feature matrix was constructed from 10 lags, corresponding to 100 ms in the past, of EEG data. The embedded time interval was chosen based on previous studies demonstrating accurate decoding of lower extremity kinematics from EEG [10,11]. The feature vector for each time point was constructed by concatenating the 11 lags (the current time point plus the 10 prior) for each channel into a single vector of length $11 \times N$, where $N$ is the number of EEG channels. To avoid the problem of missing data, the feature matrix was constructed starting at the 11th EEG sample of the trial.

EEG data are used to classify the current motor activity of the participant into one of three classes: quiet, stand-to-sit, or sit-to-stand. The true state of the participant was assessed from the linear envelope of the lower extremity EMG. To attain the envelope the EMG data was detrended, band pass filtered (15 - 300 Hz), rectified, and low pass filtered (3 Hz). A simple threshold detection algorithm identified the class as 0 (quiet), 1 (stand-to-sit), or 2 (sit-to-stand) based on the linear envelope. Classes 1 and 2 were identified as time periods when the linear envelope value exceeded three standard deviations from the mean of the quiet phase value.

### *D. Classifier Optimization*

The parameters of the LFDA-GMM classifier ($k_{nn}$ and the dimensionality of the projected subspace ($r$)) were optimized for each subject using a set of training and testing data randomly selected from each class. This optimization was performed using a grid search technique while varying the values of $k_{nn}$ and $r$ from 1-99 and 1-100, respectively. Mutually exclusive training and testing data sets for optimization were randomly selected from each class. For the optimization, the number of samples selected from each class was equal for both training and testing (50% of the least populated class). The LFDA-GMM classifier was then trained and tested at all points of the parameter space for $k_{nn}$ and $r$. The optimal parameter set for each subject was selected as the one that produced the highest overall accuracy from the testing data set.

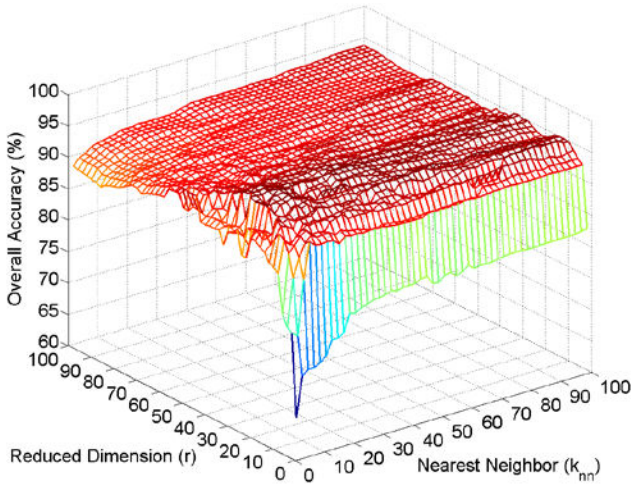


Fig. 1: A representative example (S5) of overall LFDA-GMM accuracy for optimization of parameters $r$ and $k_{nn}$.

### D. Classifier Performance

The performance of the LFDA-GMM classifier with the optimal parameter set was analyzed for each subject by randomly selecting a subset of data points to serve as the training set. The number of samples in the training subset was equal to 20% of the least populated class. After training, the LFDA-GMM classifier was then tested on all data remaining in the set for that given subject. To avoid training bias, the experiment was repeated 20 times and the accuracy reported is the average classification accuracy. We also investigated the effect of the size of the training data set by varying the size of the training set between 10%-90% of the least populated class.

## III. Results

A representative optimization surface of overall classifier accuracy as a function of parameters $k_{nn}$ and $r$ is given in Fig. 1. The contour was similar for all subjects. Accuracy plateaus at moderate $r$ values (~15-40). In some subjects, accuracy remained nearly constant for increasing values of $r$ while in other cases accuracy dipped slightly as $r$ increased beyond 40. Generally, the value of $k_{nn}$ had little impact on accuracy beyond a peak at ~11. The optimized LFDA-GMM parameters for each subject are given in Table I. The number of components ($K$), estimated from BIC, demonstrate that stand-to-sit (class 1) and sit-to-stand (class 2) distributions are multi-modal for at least half of the participants.

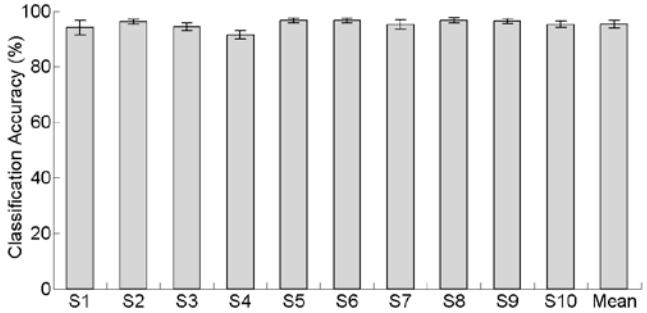


Fig. 2: Average (n = 20) LFDA-GMM classifier accuracy across subjects.

TABLE I
OPTIMAL PARAMETERS AND NUMBER OF MIXTURE COMPONENTS BY SUBJECT

| Subject | $k_{nn}$ | Reduced Dimension ($r$) | Mixture Components ($K$) | | |
|---|---|---|---|---|---|
| | | | Class 0 | Class 1 | Class 2 |
| S1 | 41 | 19 | 1 | 2 | 1 |
| S2 | 11 | 21 | 2 | 2 | 2 |
| S3 | 57 | 15 | 1 | 2 | 3 |
| S4 | 97 | 37 | 1 | 1 | 1 |
| S5 | 35 | 25 | 1 | 3 | 7 |
| S6 | 25 | 43 | 1 | 2 | 1 |
| S7 | 33 | 39 | 1 | 1 | 1 |
| S8 | 37 | 71 | 1 | 1 | 3 |
| S9 | 23 | 35 | 1 | 1 | 1 |
| S10 | 29 | 45 | 1 | 1 | 1 |

Fig. 2 shows the average classification accuracy with the optimal parameter set for each subject. The mean accuracy across the ten subjects was 95.2 ± 1.3%. Fig. 3 shows a representative example of the LFDA-GMM classifier performance for 65 seconds of the sit-to-stand and stand-to-sit experimental protocol, including the true class, predicted class, and EMG envelope of the left vastus lateralis.

## IV. Discussion

Previous studies have shown promising results for decoding of lower extremity kinematics during walking activity [10,11]. These studies and others from upper extremity [6-9] demonstrate that critical information pertaining to limb motion can be extracted from smooth amplitude modulated brain waves in the delta band (0.1 – 4 Hz). Collectively, these studies show that limb motion can be reconstructed from EEG. Such reconstruction could be used as a control signal for a noninvasive BMI for restoration of movement. However, we postulate that state-based EEG classifiers, serving as a BMI with a robotic exoskeleton or other assistive device, can provide functional recovery of movement to impaired individuals. This study shows that time-domain EEG signals from the lower delta band can be effectively used to classify movement state in healthy individuals with a very high level of accuracy, providing impetus for its use in a BMI.

Our underlying hypothesis for this study was that because spatially coarse EEG signals are combinations of many neural sources, the within-class statistical distribution of data can be multi-modal, and thus a classification scheme that can handle such non-Gaussian distributions will accurately classify the movement state. The results presented support this hypothesis. Optimization of classifier parameters for each subject is critical. For every subject peak accuracy was attained in a reduced dimensional space of less than 25% of the original, indicating LFDA was able to significantly reduce dimensionality while preserving the statistical features necessary for accurate classification. Furthermore, the GMMs for the stand-to-sit (class 1) and sit-to-stand (class 2) classes contain more than one mixture component for over half the subjects, supporting our assumption of multi-modal within class data.

In a similar manner as previous studies [15], we introduced a control group during classifier optimization to

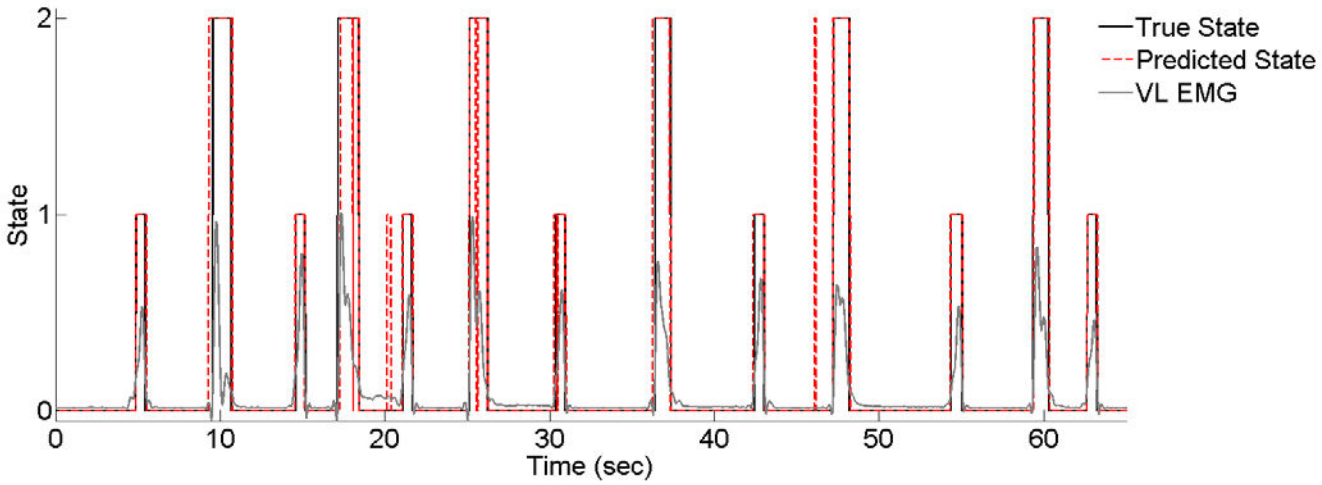


Fig. 3: Representative example of LFDA-GMM classification of user action from EEG: quiet (0), stand-to-sit (1), or sit-to-stand (2). Predicted and true states of the participant are shown with the EMG of left vastus lateralis (VL) as a reference.

strengthen our conclusion regarding classification accuracy. The control group was created by randomly shuffling original EEG data within each channel for each subject. The highest overall accuracy for LFDA-GMM optimization was significantly higher for original EEG than control ($p < 10^{-6}$). Across subjects, the maximum accuracy during optimization for the control EEG was 35.5 ± 5.8 %, which does not compare favorably to chance value of 33%.

We also found that training set size had little impact on classifier performance. Even when trained using a set of length equal to 10% of the least populated class (comprising approximately 2% of the total data set), mean accuracy was 88.7 ± 6.4 % across subjects. The length of the 10% training set was 7.8$N$ on average, where $N$ is the size of the original feature space (number of EEG channels). This finding agrees with previous studies of LFDA-GMM classifiers that found similar accuracy levels at the same training abundance [12]. Furthermore, these high accuracies with relatively low number of training samples demonstrate robustness of the LFDA-GMM classifier to EEG artifacts since the training data are taken randomly in time from each class.

In this study, LFDA-GMM demonstrated high accuracy for prediction of current motor state during one experimental session. For real time application, within-class statistical data distribution can be expected to vary between sessions, and thus the classifier may need to be optimized before each use. Despite feature reduction by LFDA, the optimal parameter set (Table I) can still result in a relatively large learning space for the GMMs as described in section II. This is a potential hindrance for real-time deployment of this classifier. However, careful examination of subject specific surfaces like the one in Fig. 2 shows that gains in accuracy level-off at values of approximately 20 and 11 for $r$ and $k_{nn}$, respectively, with only small gains in accuracy for parameters exceeding these levels. These results suggest online application of the LFDA-GMM classifier to be reasonable. Future work will focus on its implementation in combination with a robotic exoskeleton [16].

## REFERENCES


[1] J.J. Daly, J.R. Wolpaw, "Brain-computer interfaces in neurological rehabilitation," *Lancet Neurol.*, vol. 7, no. 11, pp.1032-1043, 2008.

[2] K. Gramann, J.T. Gwin, et al., "Cognition in action: imaging brain/ body dynamics in mobile humans," *Rev. Neurosci.*, vol. 22, no. 6, pp. 593-608, 2011.

[3] M.A. Lebedev, A.J. Tate, et al., "Future developments in brain-machine interface research," *Clinics*, vol. 66, no. S1, pp. 25-32, 2011.

[4] A. Bashashati, M. Fatourechi, et al., "A survey of signal processing algorithms in brain-computer interfaces based on electrical brain signals," *J. Neural. Eng.*, vol. 4, no. 2, pp. R32-R57, 2007.

[5] J.M. Carmena, M.A. Lebedev, et al., "Learning to control a brain-machine interface for reaching and grasping by primates," *PLoS Biol.*, vol. 1, no. 2, pp. e42, 2003.

[6] S. Acharya, M.S. Fifer, et al., "Electrocorticographic amplitude predicts finger positions during slow grasping motions of the hand," *J Neural. Eng.*, vol. 7, no. 4, pp. 046002, 2010.

[7] N.F. Ince, R. Gupta, et al., "High accuracy decoding of movement target direction in non-human primates based on common spatial patterns of local field potentials," *PLoS One*, vol. 5, no. 12, pp. e14384, 2010.

[8] T.J. Bradberry, R.J. Gentili, and J.L. Contreras-Vidal, "Reconstructing three-dimensional hand movements from noninvasive electroencephalographic signals," *J. Neurosci.*, vol. 30, no. 9, pp. 3432-3437, 2010.

[9] A. Muralidharan, J. Chae, and D.M. Taylor, "Extracting attempted hand movements from EEGs in people with complete hand paralysis following stroke," *Frontiers in NeuroSci.*, vol. 5, no. 39, 2011.

[10] A. Presacco, R. Goodman, L. Forrester, and J.L. Contreras-Vidal, "Neural decoding of treadmill walking from noninvasive electroencephalographic (EEG) signals," *J. Neurophysiol.*, vol. 106, pp. 1875-1887, 2011.

[11] A. Presacco, L.W. Forrester, J.L. Contreras-Vidal, "Decoding intra-limb and inter-limb kinematics during treadmill waling from scalp electroencephalographic (EEG) signals," *IEEE Trans. Neur. Sys. Rehab.*, vol. 20, no. 2, pp. 212-219, 2011.

[12] W. Li, S. Prasad, et al., "Locality-preserving dimensionality reduction and classification for hyperspectral image analysis," *IEEE Trans. Geosci. Remote Sens.*, vol. 50, no. 4, pp. 1185-1198, 2012.

[13] N. Vlassis, A. Likas, "A greedy EM algorithm for Gaussian mixture learning," *Neural Proc. Let.,* vol. 15, no. 1, pp. 77-87, 2002.

[14] T.C. Bulea, A. Kilicarslan, R. Ozdemir, W.H. Paloski, and J.L. Contreras-Vidal, "Simultaneous electroencephalography (EEG), electromyography (EMG), and whole-body segmental inertial recording for multi-modal neural decoding," *J. Vis. Exp.*, in press.

[15] J. Liu, C. Perdoni, and Bin He, "Hand movement by phase-locking low frequency EEG signals," *Proc. IEEE Eng. Med. Biol. Soc.,* pp. 6335-6338, 2011.

[16] A. Kilicarslan, S. Prasad, et al., "High accuracy decoding of user intentions using EEG to control a lower-body exoskeleton," *Proc. IEEE Eng. Med. Biol. Soc.,* submitted for publication, 2013.